Article

Antidepressant actions of ketamine engage cell-specific translation via eIF4E

https://doi.org/10.1038/s41586-020-03047-0

Received: 3 July 2019

Accepted: 27 October 2020

Published online: 16 December 2020

Check for updates

Argel Aguilar-Valles[1,2,3,6]✉, Danilo De Gregorio[1,4], Edna Matta-Camacho[1,3], Mohammad J. Eslamizade[1,2], Abdessattar Khlaifia[2], Agnieszka Skaleka[1], Martha Lopez-Canul[4], Angelica Torres-Berrio[5], Sara Bermudez[1], Gareth M. Rurak[3], Stephanie Simard[3], Natalina Salmaso[3], Gabriella Gobbi[4], Jean-Claude Lacaille[2,6] & Nahum Sonenberg[1,6]✉

Effective pharmacotherapy for major depressive disorder remains a major challenge, as more than 30% of patients are resistant to the first line of treatment (selective serotonin reuptake inhibitors)[1]. Sub-anaesthetic doses of ketamine, a non-competitive *N*-methyl-D-aspartate receptor antagonist[2,3], provide rapid and long-lasting antidepressant effects in these patients[4–6], but the molecular mechanism of these effects remains unclear[7,8]. Ketamine has been proposed to exert its antidepressant effects through its metabolite (2R,6R)-hydroxynorketamine ((2R,6R)-HNK)[9]. The antidepressant effects of ketamine and (2R,6R)-HNK in rodents require activation of the mTORC1 kinase[10,11]. mTORC1 controls various neuronal functions[12], particularly through cap-dependent initiation of mRNA translation via the phosphorylation and inactivation of eukaryotic initiation factor 4E-binding proteins (4E-BPs)[13]. Here we show that 4E-BP1 and 4E-BP2 are key effectors of the antidepressant activity of ketamine and (2R,6R)-HNK, and that ketamine-induced hippocampal synaptic plasticity depends on 4E-BP2 and, to a lesser extent, 4E-BP1. It has been hypothesized that ketamine activates mTORC1–4E-BP signalling in pyramidal excitatory cells of the cortex[8,14]. To test this hypothesis, we studied the behavioural response to ketamine and (2R,6R)-HNK in mice lacking 4E-BPs in either excitatory or inhibitory neurons. The antidepressant activity of the drugs is mediated by 4E-BP2 in excitatory neurons, and 4E-BP1 and 4E-BP2 in inhibitory neurons. Notably, genetic deletion of 4E-BP2 in inhibitory neurons induced a reduction in baseline immobility in the forced swim test, mimicking an antidepressant effect. Deletion of 4E-BP2 specifically in inhibitory neurons also prevented the ketamine-induced increase in hippocampal excitatory neurotransmission, and this effect concurred with the inability of ketamine to induce a long-lasting decrease in inhibitory neurotransmission. Overall, our data show that 4E-BPs are central to the antidepressant activity of ketamine.

A single sub-anaesthetic dose of ketamine elicits a rapid (within hours) and sustained (up to seven days) antidepressant response in patients with treatment-resistant major depressive disorder (MDD)[4–6], serving as the basis for the approval of the enantiomer (*S*)-ketamine (esketamine) by the FDA for treatment of MDD. Ketamine may exert its antidepressant effects via one of its metabolites, (2R,6R)-HNK[9], which may act as an inhibitor of NMDA (*N*-methyl-D-aspartate) receptors at certain concentrations[9,15,16]. Ketamine and (2R,6R)-HNK activate mTORC1 signalling and protein synthesis in the prefrontal cortex (PFC) and hippocampus (HPC)[7,10,11,17–20]. Furthermore, in rodents, the antidepressant response to ketamine and (2R,6R)-HNK is blocked by infusion of rapamycin, an allosteric inhibitor of mTORC1, into the PFC[10,11]. mTORC1 affects cellular functions as diverse as nucleotide and lipid synthesis, glucose metabolism, autophagy, lysosome biogenesis, proteasome assembly, and 5′-cap-dependent mRNA translation[12,13]. Therefore, it is important to understand the specific mechanism by which ketamine induces its antidepressant effect.

Members of the 4E-BP family are pivotal mTORC1 effectors that control mRNA translation (protein synthesis)[21]. The 4E-BP partner, eIF4E, binds to the mRNA 5′-cap structure (m7GpppN, where N is any nucleotide) as a protein complex termed eIF4F, which mediates the recruitment of the ribosome[13]. Hypophosphorylated 4E-BPs bind

[1]Department of Biochemistry and Goodman Cancer Centre, McGill University, Montreal, Quebec, Canada. [2]Department of Neurosciences and Centre for Interdisciplinary Research on Brain and Learning, Université de Montréal, Montreal, Quebec, Canada. [3]Department of Neuroscience, Carleton University, Ottawa, Ontario, Canada. [4]Department of Psychiatry, McGill University, Montreal, Quebec, Canada. [5]Nash Family Department of Neuroscience, Friedman Brain Institute, Icahn School of Medicine at Mount Sinai, New York, NY, USA. [6]These authors jointly supervised this work: Argel Aguilar-Valles, Jean-Claude Lacaille, Nahum Sonenberg. ✉e-mail: argel.aguilavalles@carleton.ca; nahum.sonenberg@mcgill.ca

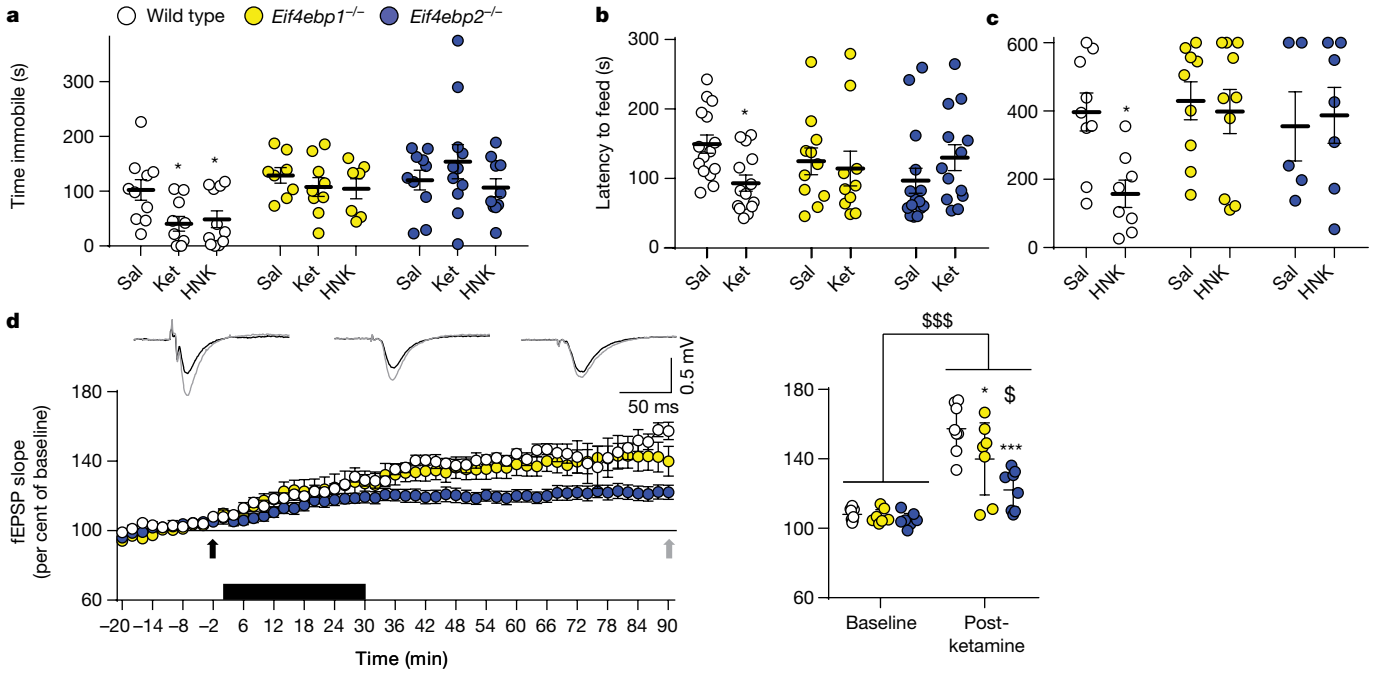

Fig. 1 | 4E-BP1 and 4E-BP2 are required for the antidepressant effect of ketamine. a, Time immobile in the FST for wild-type, *Eif4ebp1*$^{-/-}$ and *Eif4ebp2*$^{-/-}$ mice treated with saline (Sal), ketamine (Ket) or (2R,6R)-HNK (HNK) and tested 1 h after treatment (two-way ANOVA, Fisher's LSD, $n = 10, 10, 11, 8, 9, 7, 10, 11, 10$ from left to right). **b**, NSF performance of mice treated with saline or ketamine (two-way ANOVA, Fisher's LSD, $n = 15, 14, 11, 10, 15, 13$ from left to right). **c**, NSF performance of mice treated with saline or (2R,6R)-HNK (two-way ANOVA, Fisher's LSD, $n = 9, 8, 9, 10, 5, 7$ from left to right). **d**, Left, Slopes of CA1 fEPSPs recorded in slices from wild-type, *Eif4ebp1*$^{-/-}$ and *Eif4ebp2*$^{-/-}$ mice during treatment with ketamine (black bar indicates time of ketamine treatment). Top left, representative traces before (−2 min, black) and 90 min after (grey) application of ketamine (arrows indicate times of traces). Right, comparison of fEPSP slope before (−2 min) and 90 min after treatment with ketamine (two-way ANOVA, Bonferroni's test, $n = 8, 7, 8$, from left to right). Mean ± s.e.m.; $^{*}P < 0.05$, $^{***}P < 0.001$ versus saline-treated wild-type mice (**a**–**c**) or versus post-ketamine wild-type mice (**d**); $^{\$}P < 0.05$ versus post-ketamine *Eif4ebp1*$^{-/-}$ mice; $^{\$\$\$}P < 0.001$ main effect of treatment.

eIF4E to prevent the formation of eIF4F, thus impeding the initiation of mRNA translation. Following phosphorylation by mTORC1, 4E-BPs dissociate from eIF4E, thus promoting mRNA translation initiation[21]. The mTORC1–4E-BP signalling axis is crucial for synaptic plasticity[21].

There are three 4E-BP-encoding genes in mammals. The most abundant isoform in the mouse brain is 4E-BP2[22], but the presence of 4E-BP1 has also been documented[21]. Before examining the consequences of ablation of 4E-BP genes on behaviours (Fig. 1), we confirmed the expression of 4E-BP1 and 4E-BP2 in the adult mouse PFC and HPC (Extended Data Fig. 1a). To our knowledge, the distribution of 4E-BP1 and 4E-BP2 in different types of brain cells has not been investigated. In the HPC, neurons (CAMK2α^{+} and GAD67^{+}) expressed only 4E-BP2 (Extended Data Fig. 1b, c), whereas 4E-BP1 was restricted to astrocytes and microglia (Extended Data Fig. 1d–f). By contrast, in the PFC, 4E-BP1 and 4E-BP2 were expressed in excitatory (CAMK2α^{+}) and inhibitory (GAD67^{+}) neurons (Figs. 2a, b, e, f).

The effect of ketamine requires 4E-BPs

We injected (*R*,*S*)-ketamine (10 mg kg^{-1}) or saline intraperitoneally (IP) into mice lacking 4E-BP1 (*Eif4ebp1*$^{-/-}$) or 4E-BP2 (*Eif4ebp2*$^{-/-}$) and their wild-type littermates and evaluated their performance in the forced swim test (FST). In wild-type mice, ketamine induced a decrease in immobility at 1 h (by 67.9%, Fig. 1a), 24 h (by 47.8%, Extended Data Fig. 2a), and 144 h (by 55.1%, Extended Data Fig. 2b) after injection. By contrast, ketamine did not induce any change in immobility in either *Eif4ebp1*$^{-/-}$ or *Eif4ebp2*$^{-/-}$ mice at any of the time points (Fig. 1a, Extended Data Fig. 2a, b). Even a higher dose of ketamine (30 mg kg^{-1}, IP), which reduced immobility by 80.6% in wild-type mice six days after injection, did not decrease immobility in 4E-BP1 or 4E-BP2 mutant mice (Extended Data Fig. 2b).

To determine whether the antidepressant function of the ketamine metabolite (2R,6R)-HNK also depends on 4E-BPs, we treated *Eif4ebp1*$^{-/-}$ and *Eif4ebp2*$^{-/-}$ mice and their wild-type littermates with saline or (2R,6R)-HNK (20 mg kg^{-1}, IP). Injection of (2R,6R)-HNK induced a 61.1% reduction in immobility in wild-type mice, but not in *Eif4ebp1*$^{-/-}$ or *Eif4ebp2*$^{-/-}$ mice (Fig. 1a). By contrast, a single dose of fluoxetine, a selective serotonin reuptake inhibitor (SSRI; 3 mg kg^{-1}, IP; 0.5 h before testing), which reduces immobility in the FST, was similarly effective in wild-type, *Eif4ebp1*$^{-/-}$ and *Eif4ebp2*$^{-/-}$ mice (Extended Data Fig. 2h). Treatments with ketamine or (2R,6R)-HNK did not alter the distance travelled in an open field in wild-type, *Eif4ebp1*$^{-/-}$ or *Eif4ebp2*$^{-/-}$ mice (Extended Data Fig. 2c), indicating that potential differences in locomotion did not influence the FST results.

To corroborate these results, we tested mice in the novelty-suppressed feeding (NSF) task. In wild-type mice, ketamine reduced the latency to feed in a novel environment by 37.5% one hour after administration (Fig. 1c), without affecting the latency to feed in the home cage (Extended Data Fig. 2d). By contrast, in *Eif4ebp1*$^{-/-}$ and *Eif4ebp2*$^{-/-}$ mice, ketamine did not affect the latency to feed in the novel environment (Fig. 1c). Similarly, (2R,6R)-HNK reduced the latency to feed in a novel context in wild-type mice (by 61.1%), but not in *Eif4ebp1*$^{-/-}$ or *Eif4ebp2*$^{-/-}$ mice (Fig. 1c), without affecting the latency to feed in the home cage (Extended Data Fig. 2e) or locomotion during the NSF test (Extended Data Fig. 2f). Furthermore, ketamine reduced immobility in the tail suspension test (TST) in wild-type mice (by 17.0%), but not in *Eif4ebp1*$^{-/-}$ or *Eif4ebp2*$^{-/-}$ mice (Extended Data Fig. 2g).

Ketamine induces synaptic plasticity, which can be blocked by AMPA (α-amino-3-hydroxy-5-methyl-4-isoxazolepropionic acid) receptor antagonists[9,10,23]. To determine whether potentiation of excitatory synaptic transmission in the HPC was impaired in *Eif4ebp1*$^{-/-}$ and

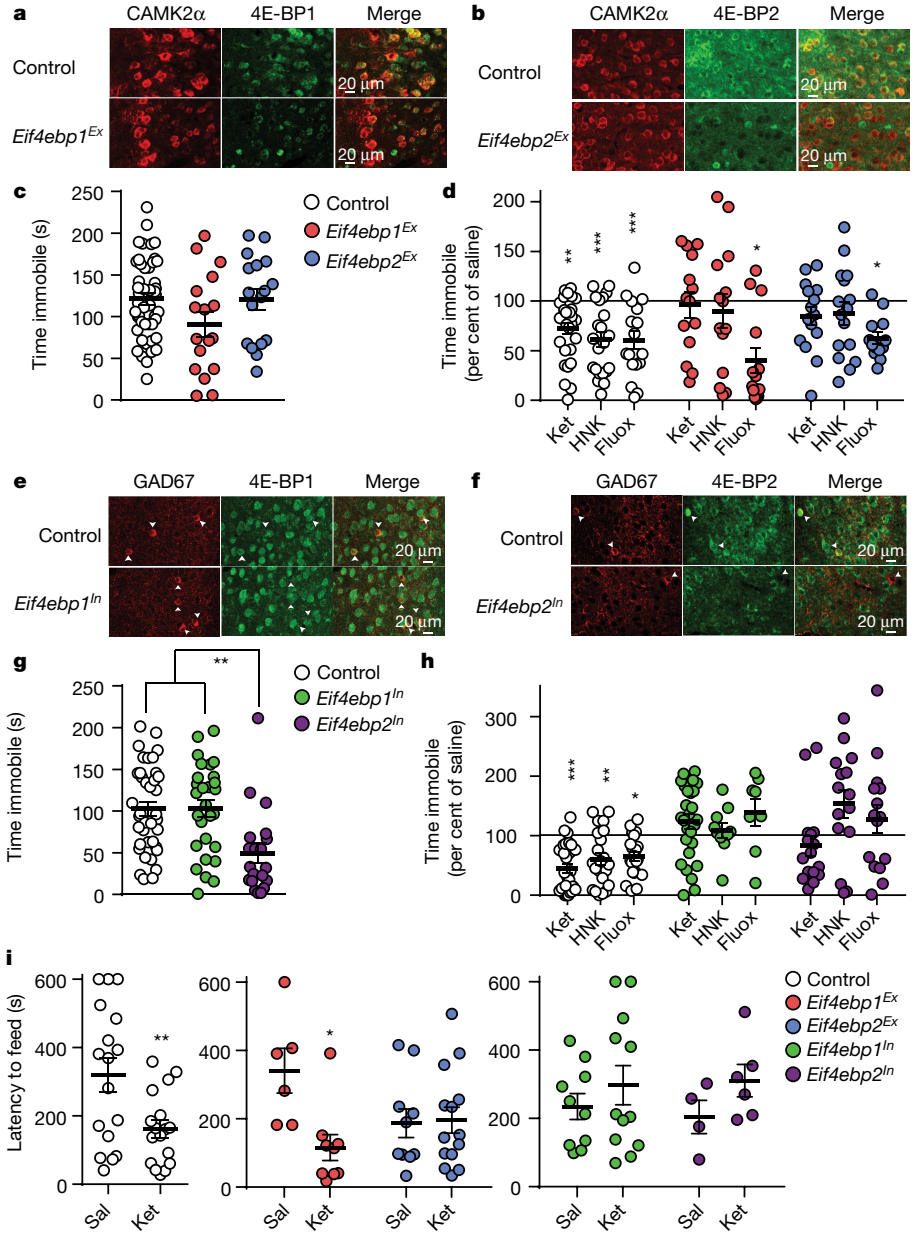

Fig. 2 | Differential effects of 4E-BP1 and 4E-BP2 in neuronal populations in response to ketamine and (2R,6R)-HNK. a, Immunostaining for CAMK2α and 4E-BP1 in the medial PFC of control and *Eif4ebp1*^{Ex} mice (representative of $n = 3$). **b**, Immunostaining for CAMK2α and 4E-BP2 in control and *Eif4ebp2*^{Ex} mice ($n = 3$). **c**, Time immobile in the FST for saline-treated control, *Eif4ebp1*^{Ex} and *Eif4ebp2*^{Ex} mice (1 h; one-way ANOVA, $n = 47, 17, 17$ from left to right). **d**, Effects of ketamine, (2R,6R)-HNK and fluoxetine (Fluox) on time immobile in the FST (shown as percentage of time immobile with saline treatment; one-way ANOVA and Dunnett's test, $n = 29, 22, 17, 14, 14, 14, 15, 16, 13$ from left to right). **e**, Immunostaining for GAD67 and 4E-BP1 in the medial PFC of control and *Eif4ebp1*^{In} mice ($n = 3$). **f**, GAD67 and 4E-BP2 immunohistochemistry in control and *Eif4ebp2*^{In} mice ($n = 3$). **g**, Time immobile in the FST for saline-treated control, *Eif4ebp1*^{In} and *Eif4ebp2*^{In} mice (one-way ANOVA and Tukey's test, $n = 38, 28, 20$ from left to right). **h**, Effects of ketamine, (2R,6R)-HNK and fluoxetine on time immobile in the FST in control, *Eif4ebp1*^{In} and *Eif4ebp2*^{In} mice (one-way ANOVA and Dunnett's test, $n = 30, 22, 21, 28, 10, 8, 16, 15, 15$ from left to right). **i**, Effects of ketamine on NSF in control, *Eif4ebp1*^{Ex}, *Eif4ebp2*^{Ex}, *Eif4ebp1*^{In} and *Eif4ebp2*^{In} mice (two-way ANOVA, Fisher's LSD, $n = 17, 17, 6, 9, 10, 14, 10, 12, 4, 6$ from left to right). Mean ± s.e.m.; $^{*}P < 0.05$, $^{**}P < 0.01$, $^{***}P < 0.001$ versus saline-treated mice.

Eif4ebp2$^{-/-}$ mice, we treated hippocampal slices from these and wild-type mice with ketamine (20 μM for 30 min; Fig. 1d). Ketamine increased the slope of field excitatory postsynaptic potentials (fEPSPs) in hippocampal region CA1 in all three strains, but it was larger in wild-type mice than in *Eif4ebp1*$^{-/-}$ mice (by 17.43%) or *Eif4ebp2*$^{-/-}$ mice (by 35.26%) (Fig. 1d). Consistent with the neuronal expression of 4E-BP2 in the HPC (Extended Data Fig. 1b–f), attenuation of ketamine-induced fEPSP potentiation was greater in *Eif4ebp2*$^{-/-}$ mice than in *Eif4ebp1*$^{-/-}$ mice (by 17.86%) or wild-type mice. Overall, these results demonstrate that both 4E-BPs contribute to the synaptic and behavioural effects of ketamine in mice.

Mutation of 4E-BPs in excitatory neurons

Ketamine may act directly on excitatory cortical neurons, or on inhibitory interneurons to increase excitability[10,14,23,24], leading to the activation of mTORC1 in excitatory neurons[14]. To test whether 4E-BPs are required in excitatory or inhibitory neurons, we generated cell-specific deletions of *Eif4ebp1* and *Eif4ebp2* (Extended Data Fig. 3). Mice deficient for either 4E-BP1 or 4E-BP2 in excitatory neurons (*Eif4ebp1*^{Ex} or *Eif4ebp2*^{Ex}; Fig. 2a, b) showed no change in immobility in the FST compared to control mice (Fig. 2c). We treated the mice with ketamine,

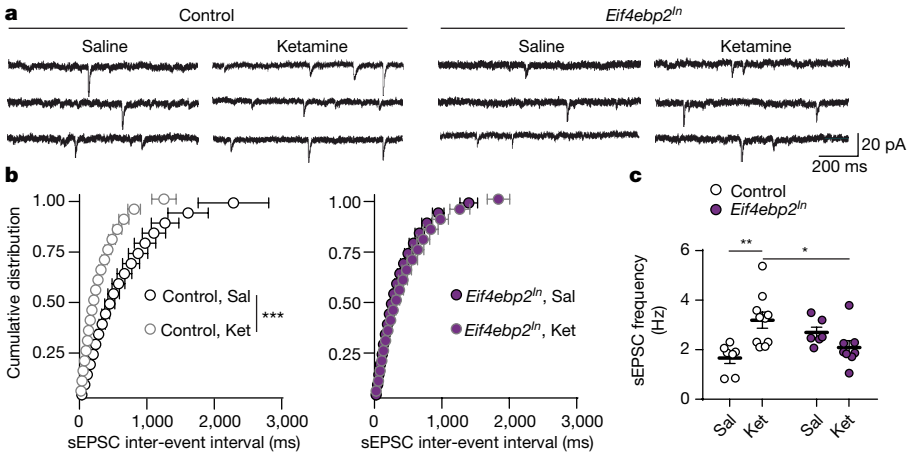

Fig. 3 | Ketamine-induced increase in excitatory synaptic transmission in pyramidal cells depends on the expression of 4E-BP2 in inhibitory neurons. **a**, Whole-cell recordings of sEPSCs in CA1 pyramidal neurons, 24 h after treatment with saline or ketamine in control or *Eif4ebp2*^{In} mice. **b**, Cumulative distributions of sEPSC inter-event intervals as in **a** (Kolmogorov–Smirnov test, $n = 7, 10, 6, 8$ from left to right). **c**, Frequencies of sEPSCs as in **a** (two-way ANOVA and Bonferroni's test). Mean ± s.e.m.; $^{*}P < 0.05$, $^{**}P < 0.01$, $^{***}P < 0.001$.

(2R,6R)-HNK or fluoxetine. Control mice responded to ketamine or (2R,6R)-HNK with a decrease in immobility in the FST (ketamine, 27.6%; (2R,6R)-HNK, 39% reduction; Fig. 2d). Consistent with the premise that ketamine stimulates mRNA translation in excitatory neurons, mice deficient for either 4E-BP1 or 4E-BP2 in excitatory neurons showed no response to either ketamine or (2R,6R)-HNK (Fig. 2d). Notably, fluoxetine reduced immobility in the FST in control (39.4%), *Eif4ebp1*^{Ex} (60.2%) and *Eif4ebp2*^{Ex} mice (37.7% reduction; Fig. 2d), showing that the acute response to SSRIs (the actions of which are mechanistically distinct from those of ketamine) does not require the 4E-BPs in glutamatergic neurons.

Deletion of 4E-BPs in inhibitory neurons

Dysregulation of GABA (γ-aminobutyric acid)-mediated neurotransmission contributes to the pathophysiology of MDD, and the effect of ketamine on these neurons has been proposed to be central in eliciting antidepressant responses[25–27]. Consistent with this, mice lacking 4E-BP2 in GAD2^{+} inhibitory neurons (*Eif4ebp2*^{In}, generated using *Gad2-Cre* mice; Fig. 2e, f) showed decreased immobility when treated with saline (Fig. 2g) compared to wild-type or *Eif4ebp1*^{In} mice. Furthermore, lack of 4E-BP1 or 4E-BP2 in *Gad2*-expressing cells conferred resistance to ketamine and (2R,6R)-HNK (Fig. 2h), and even to the acute effects of fluoxetine (Fig. 2h).

To determine whether the long-lasting effect of ketamine was also occluded in mice with cell-specific mutations of *Eif4ebp1* and *Eif4ebp2*, we measured immobility in the FST six days after treatment with saline or ketamine (Extended Data Fig. 4c). Similar to the one-hour time point, ketamine decreased immobility only in control mice, and not in *Eif4ebp1*^{Ex}, *Eif4ebp2*^{Ex}, *Eif4ebp1*^{In} or *Eif4ebp2*^{In} mice (Extended Data Fig. 4c). In addition, in *Eif4ebp2*^{Ex}, *Eif4ebp1*^{In} and *Eif4ebp2*^{In} mice, ketamine did not decrease the latency to feed in a novel environment, although it did in control and *Eif4ebp1*^{Ex} mice (Fig. 2i). Neither treatment nor genotype altered latency to feed in the home cage (Extended Data Fig. 4a) or locomotion during the NSF test (Extended Data Fig. 4b). Thus, 4E-BP1 and 4E-BP2 in inhibitory neurons are required for the acute and sustained effects of ketamine; this highlights the importance of inhibitory neuronal circuit elements in the treatment of depression.

The absence of 4E-BP2 in inhibitory neurons resulted in diminished immobility in the FST (Fig. 2g); we therefore studied the role of 4E-BP2 in inhibitory neurons using patch-clamp recordings from hippocampal

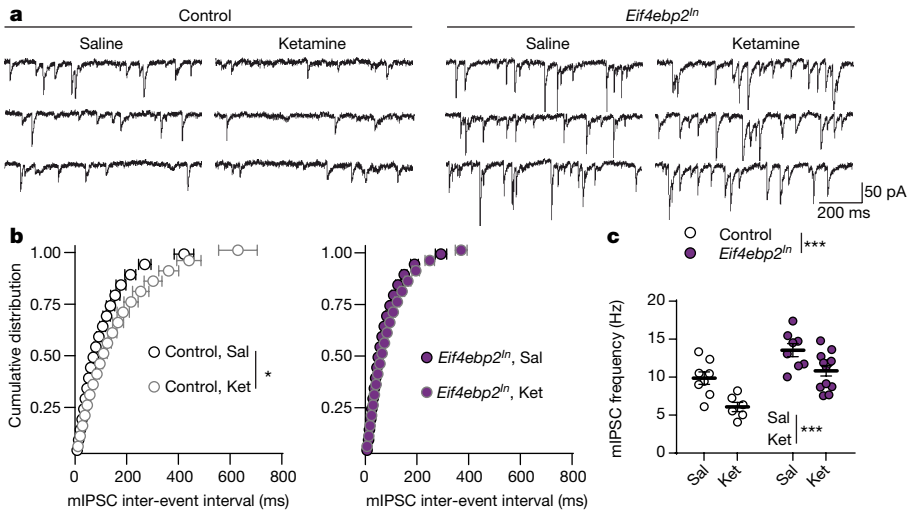

Fig. 4 | Inhibitory synaptic transmission in pyramidal cells and its depression by ketamine depend on the expression of 4E-BP2 in inhibitory interneurons. **a**, Recordings of mIPSCs from CA1 pyramidal neurons of control and *Eif4ebp2*^{In} mice 24 h after treatment with saline or ketamine. **b**, Cumulative distributions of mIPSC inter-event intervals (Kolmogorov–Smirnov test, $n = 8, 6, 8, 12$ from left to right). **c**, Frequencies of CA1 mIPSCs (two-way ANOVA). Mean ± s.e.m.; $^{*}P < 0.05$, $^{***}P < 0.001$.

slices. First, we measured spontaneous excitatory postsynaptic currents (sEPSCs) in CA1 pyramidal neurons in slices, 24 h after treatment of mice with saline or ketamine (IP, 10 mg kg^{-1}), to capture the long-lasting plasticity elicited by in vivo treatment (Fig. 3). In control mice, ketamine induced an increase in the frequency of sEPSCs (Fig. 3a–c), but not in their amplitude (Fig. 3a, Extended Data Fig. 5a, b). By contrast, this effect was absent in slices from *Eif4ebp2*^{ln} mice (Fig. 3a–c). We then studied correlative changes in miniature EPSCs (mEPSCs) and inhibitory postsynaptic currents (mIPSCs) in CA1 pyramidal neurons from control and *Eif4ebp2*^{ln} mice. The frequency and amplitude of mEPSCs were not altered by either treatment or genotype (Extended Data Fig. 6a–e). By contrast, the frequency of mIPSCs was increased in slices from *Eif4ebp2*^{ln} mice (Fig. 4a–c) and decreased by ketamine in CA1 pyramidal neurons from control mice (Fig. 4a, b). Moreover, the decrease induced by ketamine in control mice was absent in *Eif4ebp2*^{ln} mice (Fig. 4a–c). Neither treatment nor genotype affected the amplitude of mIPSCs (Extended Data Fig. 5c, d). These data indicate that long-lasting depression of inhibitory synaptic transmission by ketamine contributes to the elevated excitatory synaptic responses in CA1 pyramidal neurons in control mice.

In summary, we have shown that the mTORC1 effectors 4E-BP1 and 4E-BP2 are necessary for the antidepressant response to ketamine (in the FST, NSF test and TST; Figs. 1, 2, Extended Data Fig. 2) and for synaptic plasticity in the HPC (Figs. 1, 3, 4). The ketamine metabolite (2R,6R)-HNK was also ineffective in mice lacking 4E-BP1 or 4E-BP2 (Figs. 1, 2). The 4E-BPs are important for synaptic transmission and for the induction of synaptic and structural plasticity[21], such as that induced by ketamine in the HPC (Figs. 1e, 3, 4), the PFC[10,28] and the lateral habenula[29]. Furthermore, the absence of 4E-BP2 has been shown to increase the frequency and amplitude of mEPSCs and the amplitude of mIPSCs in pyramidal CA1 neurons[30,31], indicating that this signalling axis is involved in pre- and postsynaptic mechanisms to control the activity of both excitatory and inhibitory neurons. Activation of 4E-BP2 in excitatory neurons and of both 4E-BP1 and 4E-BP2 in inhibitory neurons is an absolute requirement for the antidepressant response to ketamine (Fig. 2). This is consistent with 4E-BP2 being the most abundant 4E-BP isoform in the brain[21,22], and specifically in the HPC (Extended Data Fig. 1b–f).

Our finding that knockout of 4E-BP2 in inhibitory neurons induced a decrease in immobility in the FST supports the idea that GABAergic interneurons are important for the response to antidepressant treatments[25–27]. Indeed, the absence of 4E-BP2 in inhibitory neurons resulted in increased GABAergic synaptic transmission (Fig. 4a–c), which coincided with blocked enhancement of excitatory synaptic potentials by ketamine (Fig. 3a–c). Therefore, as part of its mechanism of action, ketamine triggers 4E-BP2-mediated plasticity events in inhibitory neurons that are likely to be central in maintaining the potentiation of excitatory synaptic transmission for days after ketamine administration.

Reduced activity in the mTORC1 signalling pathway has been identified in post-mortem tissue from individuals with MDD[32]. Thus, this pathway could be a target for treating MDD. Notably, in patients with MDD, one dose of orally administered rapamycin amplified the effect of ketamine[33]. This finding suggests the possibility that there may be divergent peripheral and central effects of rapamycin in modulating the effects of ketamine. Our results demonstrate that brain 4E-BPs, and downstream initiation of mRNA translation, are a pivotal target for ketamine and its metabolite (2R,6R)-HNK. Therefore, brain 4E-BPs are appealing targets for the treatment of depressive disorders.

Online content

Any methods, additional references, Nature Research reporting summaries, source data, extended data, supplementary information, acknowledgements, peer review information; details of author contributions and competing interests; and statements of data and code availability are available at https://doi.org/10.1038/s41586-020-03047-0.

1. Rush, A. J. et al. Acute and longer-term outcomes in depressed outpatients requiring one or several treatment steps: a STAR*D report. *Am. J. Psychiatry* **163**, 1905–1917 (2006).
2. Hirota, K. & Lambert, D. G. Ketamine: its mechanism(s) of action and unusual clinical uses. *Br. J. Anaesth.* **77**, 441–444 (1996).
3. Kashiwagi, K. et al. Channel blockers acting at *N*-methyl-D-aspartate receptors: differential effects of mutations in the vestibule and ion channel pore. *Mol. Pharmacol.* **61**, 533–545 (2002).
4. Berman, R. M. et al. Antidepressant effects of ketamine in depressed patients. *Biol. Psychiatry* **47**, 351–354 (2000).
5. Zarate, C. A., Jr et al. A randomized trial of an *N*-methyl-D-aspartate antagonist in treatment-resistant major depression. *Arch. Gen. Psychiatry* **63**, 856–864 (2006).
6. Lapidus, K. A. et al. A randomized controlled trial of intranasal ketamine in major depressive disorder. *Biol. Psychiatry* **76**, 970–976 (2014).
7. Zarate, C. A., Jr & Machado-Vieira, R. Ketamine: translating mechanistic discoveries into the next generation of glutamate modulators for mood disorders. *Mol. Psychiatry* **22**, 324–327 (2017).
8. Workman, E. R., Niere, F. & Raab-Graham, K. F. Engaging homeostatic plasticity to treat depression. *Mol. Psychiatry* **23**, 26–35 (2018).
9. Zanos, P. et al. NMDAR inhibition-independent antidepressant actions of ketamine metabolites. *Nature* **533**, 481–486 (2016).
10. Li, N. et al. mTOR-dependent synapse formation underlies the rapid antidepressant effects of NMDA antagonists. *Science* **329**, 959–964 (2010).
11. Fukumoto, K. et al. Activity-dependent brain-derived neurotrophic factor signaling is required for the antidepressant actions of (2*R*,6*R*)-hydroxynorketamine. *Proc. Natl Acad. Sci. USA* **116**, 297–302 (2019).
12. Saxton, R. A. & Sabatini, D. M. mTOR signaling in growth, metabolism, and disease. *Cell* **169**, 361–371 (2017).
13. Sonenberg, N. & Hinnebusch, A. G. Regulation of translation initiation in eukaryotes: mechanisms and biological targets. *Cell* **136**, 731–745 (2009).
14. Miller, O. H., Moran, J. T. & Hall, B. J. Two cellular hypotheses explaining the initiation of ketamine's antidepressant actions: direct inhibition and disinhibition. *Neuropharmacology* **100**, 17–26 (2016).
15. Kavalali, E. T. & Monteggia, L. M. The ketamine metabolite 2R,6R-hydroxynorketamine blocks NMDA receptors and impacts downstream signaling linked to antidepressant effects. *Neuropsychopharmacology* **43**, 221–222 (2018).
16. Suzuki, K., Nosyreva, E., Hunt, K. W., Kavalali, E. T. & Monteggia, L. M. Effects of a ketamine metabolite on synaptic NMDAR function. *Nature* **546**, E1–E3 (2017).
17. Paul, R. K. et al. (R,S)-Ketamine metabolites (R,S)-norketamine and (2S,6S)-hydroxynorketamine increase the mammalian target of rapamycin function. *Anesthesiology* **121**, 149–159 (2014).
18. Adaikkan, C., Taha, E., Barrera, I., David, O. & Rosenblum, K. Calcium/calmodulin-dependent protein kinase II and eukaryotic elongation factor 2 kinase pathways mediate the antidepressant action of ketamine. *Biol. Psychiatry* **84**, 65–75 (2018).
19. Miller, O. H., Grabole, N., Wells, I. & Hall, B. Genome-wide translating mRNA analysis following ketamine reveals novel targets for antidepressant treatment. Preprint at https://doi.org/10.1101/254904 (2018).
20. Murrough, J. W. et al. Rapid and longer-term antidepressant effects of repeated ketamine infusions in treatment-resistant major depression. *Biol. Psychiatry* **74**, 250–256 (2013).
21. Aguilar-Valles, A., Matta-Camacho, E. & Sonenberg, N. in *The Oxford Handbook of Neuronal Protein Synthesis* (ed. Wayne Sossin) (Oxford Univ. Press, 2018).
22. Banko, J. L. et al. The translation repressor 4E-BP2 is critical for eIF4F complex formation, synaptic plasticity, and memory in the hippocampus. *J. Neurosci.* **25**, 9581–9590 (2005).
23. Autry, A. E. et al. NMDA receptor blockade at rest triggers rapid behavioural antidepressant responses. *Nature* **475**, 91–95 (2011).
24. Gerhard, D. M. et al. GABA interneurons are the cellular trigger for ketamine's rapid antidepressant actions. *J. Clin. Invest.* **130**, 1336–1349 (2020).
25. Duman, R. S., Sanacora, G. & Krystal, J. H. Altered connectivity in depression: GABA and glutamate neurotransmitter deficits and reversal by novel treatments. *Neuron* **102**, 75–90 (2019).
26. Ng, L. H. L. et al. Ketamine and selective activation of parvalbumin interneurons inhibit stress-induced dendritic spine elimination. *Transl. Psychiatry* **8**, 272 (2018).
27. Widman, A. J. & McMahon, L. L. Disinhibition of CA1 pyramidal cells by low-dose ketamine and other antagonists with rapid antidepressant efficacy. *Proc. Natl Acad. Sci. USA* **115**, E3007–E3016 (2018).
28. Moda-Sava, R. N. et al. Sustained rescue of prefrontal circuit dysfunction by antidepressant-induced spine formation. *Science* **364**, eaat8078 (2019).
29. Yang, Y. et al. Ketamine blocks bursting in the lateral habenula to rapidly relieve depression. *Nature* **554**, 317–322 (2018).
30. Bidinosti, M. et al. Postnatal deamidation of 4E-BP2 in brain enhances its association with raptor and alters kinetics of excitatory synaptic transmission. *Mol. Cell* **37**, 797–808 (2010).
31. Gkogkas, C. G. et al. Autism-related deficits via dysregulated eIF4E-dependent translational control. *Nature* **493**, 371–377 (2013).
32. Jernigan, C. S. et al. The mTOR signaling pathway in the prefrontal cortex is compromised in major depressive disorder. *Prog. Neuropsychopharmacol. Biol. Psychiatry* **35**, 1774–1779 (2011).
33. Abdallah, C. et al. Rapamycin, an immunosuppressant and mTORC1 inhibitor, triples the antidepressant response rate of ketamine at 2 weeks following treatment: a double-blind, placebo-controlled, cross-over, randomized clinical trial. Preprint at https://doi.org/10.1101/500959 (2018).

Methods

Mice

Adult male mice (aged 60–180 days) were used. *Eif4ebp1*$^{-/-}$ and *Eif4ebp2*$^{-/-}$ mice have been reported[22,34]. *Eif4ebp1*$^{f/f}$ and *Eif4ebp2*$^{f/f}$ mice were generated by Ozgene Pty Ltd (Perth, Australia). To generate *Eif4ebp1*$^{f/f}$ and *Eif4ebp2*$^{f/f}$ mice, a targeting construct containing a neomycin selection cassette flanked by two short flippase recognition target (FRT) sites was used to generate a conditional allele (Extended Data Fig. 3). The targeting construct also contained two loxP sites between exons 1 and 2 and between exons 2 and 3 for both *Eif4ebp1* and *Eif4ebp2* genes (Extended Data Fig. 3). The neomycin selection cassette was removed after the generation of the 'floxed' lines. Conditional knockouts were generated by crossing *Eif4ebp1*$^{f/f}$ and *Eif4ebp2*$^{f/f}$ mice with either *Camk2a-cre* (Jackson Laboratories stock no. 005359) or *Gad2-cre* (Jackson Laboratories stock no. 010802) mice. Excitatory neuron knockout mouse lines are referred to as *Eif4ebp1*^{Ex} and *Eif4ebp2*^{Ex}; inhibitory knockout lines are *Eif4ebp1*^{In} and *Eif4ebp1*^{In}. For experiments using conditional knockout mice, control groups were a combination of either *Camk2a-cre* or *Gad2-cre*, *Eif4ebp1*$^{f/f}$, *Eif4ebp2*$^{f/f}$ and wild-type littermates. Genotyping was carried out by PCR amplification of genomic DNA from tails using the set of primers shown in Extended Data Fig. 3. For *Eif4ebp1*, amplification of wild-type genomic DNA yielded a single 250-bp PCR product, whereas *Eif4ebp1*$^{f/f}$ genomic DNA produced a 347-bp PCR product; for *Eif4ebp2*, amplification of wild-type genomic DNA yielded a single 276-bp PCR product, whereas *Eif4ebp1*$^{f/f}$ genomic DNA produced a 379-bp PCR product (Extended Data Fig. 3).

Mice were housed in groups of 2–5 per cage with free access to food and water (except in experiments involving food deprivation), in temperature- and humidity-controlled rooms (21 °C, ~55% humidity), and a 12-h light–dark cycle. All procedures followed the guidelines of the Canadian Council on Animal Care and were approved by the Animal Care Committees of McGill University and Université de Montréal.

No statistical methods were used to predetermine sample size. The experiments were not randomized, but investigators were blinded to allocation during experiments and outcome assessment.

Behavioural procedures

Mice were handled once 24 h before each experiment. All behavioural experiments were performed between 10:00 a.m. and 3:00 p.m. Behaviours were recorded, stored, and analysed as MPEG files using an automated behavioural tracking system (Videotrack, View Point Life Science, Montreal, Canada) equipped with infrared lighting-sensitive CCD cameras. The analogue signals supplied by the camera were measurements of the luminosity of each point of the image scanned point-by-point and line-by-line at a rate of 25 images per second. These signals were transmitted to the Videotrack system and digitized on 8 bits by digital analogue conversion. Before the experiments, animal–image background contrast detection thresholds were calibrated by visual inspection to distinguish different behavioural patterns.

Forced swim test. Mice were placed in a glass beaker (24 cm tall, 14 cm diameter) containing 3 l water at 24 ± 1 °C. Mice were allowed to swim for 6 min. Immobility was quantified in the last 4 min of the test using the Videotrack system. Data were expressed as percentage of immobility from saline-treated mice of the same genotype.

Tail suspension test. Mice were suspended by their tail from a lever in a 30 × 30 × 30 cm white-painted enclosure. Movements were recorded and quantified for 5 min in a dimly lit environment.

Novelty-suppressed feeding. Mice were food-deprived for 48 h, then each mouse was placed in a brightly illuminated (100 W, 350 lx) open arena (40 × 40 white-painted floor with white walls 30 cm in height) containing lab chow (three pellets) placed at the centre of the arena. The latency to initiate feeding (in seconds) and total distance travelled (cm) were measured. The cut-off time was 600 s[35]. Feeding latency was also observed in the home cage containing three pellets spread on the floor. The session was terminated immediately after the mice began to feed.

Open field. Mice were placed in a brightly illuminated (100 W, 350 lx) open arena (40 × 40 white plexiglass floors with white walls 40 cm in height) and allowed to explore for 10 min. Total distance travelled was measured (cm).

Drugs

Ketamine hydrochloride (Narketan 10, Vetoquinol) was diluted in 0.9% NaCl solution (saline) and administered IP at 10 mg kg^{-1} (in some experiments 30 mg kg^{-1} was used). Mice were tested 1, 24, or 144 h after injection. (2R,6R)-HNK (Tocris Bioscience) was diluted in saline and administered IP at 20 mg kg^{-1}; mice were tested 1 h after injection. Fluoxetine hydrochloride (Tocris Bioscience) was diluted in saline and injected IP at 3 mg kg^{-1}; mice were tested 30 min after injection.

Mouse brain collection

Wild-type, *Eif4ebp1*$^{-/-}$ and *Eif4ebp2*$^{-/-}$ mice were briefly anaesthetized using 5% isoflurane and brains were immediately removed; PFC and HPC were dissected, flash frozen and kept at −80 °C until use.

Western blotting

Tissues were homogenized in RIPA buffer and western blotting was performed as previously described[30]. Antibodies against indicated proteins were: 4E-BP1 (Cell Signaling Technology, 1:1,000), 4E-BP2 (Cell Signaling Technology, 1:1,000) and glyceraldehyde-3-phosphate dehydrogenase (GAPDH), coupled to horseradish peroxidase (1:5,000; Abcam); secondary antibody was anti-rabbit (Thermo Fisher Scientific).

Immunohistochemistry

Control, *Eif4ebp1*^{Ex}, *Eif4ebp2*^{Ex}, *Eif4ebp1*^{In} and *Eif4ebp2*^{In} adult male mice (60–120 days old) underwent transcardial fixation using phosphate-buffered saline (PBS) and then 4% paraformaldehyde. Brains were cryopreserved, flash frozen and stored at −80 °C until use. Coronal slices were prepared (30 µm) and blocked for 1 h (at room temperature) in 5% goat serum (GS) and 0.5% Triton-X in PBS. Then, slices were incubated overnight (4 °C) in 1% GS in PBS with the following antibodies: rabbit anti-4E-BP1 (Cell Signaling Technology, 1:500); rabbit anti-4E-BP2 (Cell Signaling Technology, 1:300); mouse anti-CAMKII-α (Cell Signaling Technology, 1:1,000); mouse anti-GAD67 (EMD Millipore, 1:1,000); mouse anti-GFAP (Cell Signaling Technology, 1:1,000); rat anti-CD11b (BioRad, 1:500).

Next, sections were incubated in darkness (1 h at room temperature) in blocking buffer with AlexaFluor 488 goat anti-rabbit IgG (Thermo Fisher Scientific, 1:400), AlexaFluor 546 goat anti-mouse IgG (Thermo Fisher Scientific, 1:400), AlexaFluor 647 streptavidin conjugate (Thermo Fisher Scientific) or AlexaFluor 647 goat anti-rat IgG (Thermo Fisher Scientific 1:400), and DAPI (4′,6-diamidino-2-phenylindole dihydrochloride, Life Technologies, 1:1,000). Sections were washed with PBS (3 times, 5 min each) after each incubation step. Samples were visualized using the Zeiss LSM800 laser scanning confocal microscope and Zeiss ZEN 3.2 image acquisition software.

Field recordings

For brain slice preparation, wild-type, *Eif4ebp1*$^{-/-}$ and *Eif4ebp2*$^{-/-}$ mice (60–67 days old) were anaesthetized with isoflurane and the brain was rapidly removed. Transverse hippocampal slices (400 µm thickness) were allowed to recover for at least 2 h at 32 °C submerged in oxygenated artificial cerebrospinal fluid (ACSF; 124 mM NaCl, 5 mM KCl, 1.25 mM NaH_2PO_4, 2 mM $MgSO_4$, 2 mM $CaCl_2$, 26 mM $NaHCO_3$ and 10 mM dextrose (pH 7.3–7.4; 295–300 mOsmol). After recovery,

individual slices were transferred to a submersion recording chamber and perfused at 2.5 ml/min with ACSF at 27–28 °C. Field excitatory postsynaptic potentials (fEPSPs) were recorded in CA1 stratum radiatum with glass electrodes (2–3 MΩ) filled with ASCF. Schaffer collateral fEPSPs were evoked with a concentric bipolar tungsten stimulating electrode placed in mid-stratum radiatum proximal to the CA3 region. Baseline stimulation was applied at 0.033 Hz by delivering 0.1-ms pulses, with intensity adjusted to evoke fEPSPs with 30% of maximal amplitude. After a 30-min baseline recording, ketamine was added to ACSF (20 μM) for 30 min. Recordings continued for 1 h after ketamine wash out. fEPSP slope measurements were performed on digitized analogue recordings using the Clampfit analyse function (Clampfit 10.6). The slope was measured at between 10% and 90% of maximal fEPSP amplitude during an epoch defined by constant cursor placements, which excluded fibre volley and population spikes. The experimenter was blind to the mouse genotype and codes were revealed after data analysis.

Whole-cell recording of synaptic currents

Acute hippocampal slices (300 μm thickness) were prepared in ice-cold cutting solution containing 75 mM sucrose, 87 mM NaCl, 2.5 mM NaH_2PO_4, 1.25 mM $MgSO_4$, 0.5 mM $CaCl_2$, 25 mM glucose, and 25 mM $NaHCO_3$. Slices were transferred to ACSF containing 124 mM NaCl, 2.5 mM KCl, 1.25 mM NaH_2PO_4, 24 mM $NaHCO_3$, 2 mM $MgCl_2$, 2 mM $CaCl_2$, and 12.5 mM glucose. Whole-cell recordings were obtained from CA1 pyramidal neurons using patch pipettes (borosilicate glass capillaries; 3–5 MΩ). To record EPSCs, the intracellular solution contained 120 mM $CsMeSO_4$, 5 mM CsCl, 2 mM $MgCl_2$, 10 mM HEPES, 0.5 mM EGTA (EGTA), 2 mM QX-314, 10 mM Na_2-phosphocreatine, 2 mM ATP-tris, 0.4 mM GTP-tris, and 0.1 mM spermine (pH 7.3–7.4; 285–295 mOsmol). To record IPSCs, the intracellular solution contained 135 mM CsCl, 10 mM HEPES, 2 mM QX-314, 2 mM $MgCl_2$, and 4 mM MgATP.

Recordings were obtained in voltage-clamp mode using a Multiclamp 700A amplifier (Molecular Devices). Holding potential was maintained at −70 mV and series resistance was routinely monitored. Recorded signals were low-pass-filtered at 2 kHz, digitized at 20 kHz and stored on a PC. Data acquisition and off-line analyses were performed using 1440A Digidata acquisition board, and pClamp 10 software (Molecular Devices). Data were included only if the holding current was stable or if series resistance varied by less than 25% of initial value. To record miniature events, tetrodotoxin (TTX 1 μM; Alomone Labs) was added to the ACSF. In mIPSC experiments, 6,7-dinitroquinoxaline-2,3-dione (DNQX, 20 μM) and D(−)-2-amino-5-phosphonopentanoic acid (AP5, 50 μM) were added to block excitatory transmission via AMPA and NMDA receptors. In mEPSC and sEPSC experiments, GABAzine (5 μM) was used to block $GABA_A$ receptors, and in sEPSC experiments extracellular K^+ concentration was 5 mM and TTX was omitted. For analysis, postsynaptic events were detected visually by Mini Analysis 6.0 software. The detection threshold was set at 3 pA and typically 200–300 events were sampled per neuron (range 125–200 events for EPSCs, 190–300 events for IPSCs). For the cumulative probability distribution analyses, EPSC and IPSC data were binned (bin size 5% of total number of events) for each cell to avoid oversampling from any neuron.

Statistical analyses

Data were expressed as mean ± s.e.m. and analysed using GraphPad Prism 6 (GraphPad Software Inc.). Data from Fig. 2c, d, g, h were analysed using one-way ANOVA, followed by post hoc multiple comparisons tests. Data from Figs. 1a–c, 2i, 3c, 4c, Extended Data Figs. 2a–h, 4a–c, 5b, d, 6c, e were analysed using two-way ANOVA (with treatment and genotype as factors), followed up by planned comparisons. Data from Fig. 1d were analysed using mixed-designed two-way ANOVA, with treatment time as repeated measured variable and genotype as independent variable; this was followed by Bonferroni's multiple comparisons tests. For cumulative probability distribution analyses of EPSCs and IPSCs in Figs. 3b, 4b, Extended Data Figs. 5a, c, 6b, d, data were analysed using the Kolmogorov–Smirnov test. Values of $P < 0.05$ were considered significant. Details of statistical analyses are in Supplementary Table 1.

Reporting summary

Further information on research design is available in the Nature Research Reporting Summary linked to this paper.

Data availability

All data generated and analysed during this study are included in this published Article and its Supplementary Information files. Source data are provided with this paper.

34. Tsukiyama-Kohara, K. et al. Adipose tissue reduction in mice lacking the translational inhibitor 4E-BP1. *Nat. Med.* **7**, 1128–1132 (2001).
35. Bodnoff, S. R., Suranyi-Cadotte, B., Aitken, D. H., Quirion, R. & Meaney, M. J. The effects of chronic antidepressant treatment in an animal model of anxiety. *Psychopharmacology (Berl.)* **95**, 298–302 (1988).

Acknowledgements We thank A. Sylvestre, A. Lafrance, I. Harvey and T. Degenhard for technical assistance. A.A.-V. was a recipient of FRQS (Fond Recherche Québec-Santé) and CIHR (Canadian Institutes for Health Research) postdoctoral fellowships. D.D.G. is a recipient of FRQS and CIHR postdoctoral fellowships. J.-C.L. is the recipient of the Canada Research Chair in Cellular and Molecular Neurophysiology. This work was supported by a CIHR Foundation grant to N. Sonenberg (FND-148423), and a CIHR project grant to J.-C.L. (PJT-153311).

Author contributions A.A.-V. designed the study, performed experiments, supervised students, analysed data and wrote the manuscript. D.D.G. performed behavioural experiments and data analyses. E.M.-C. performed western blot experiments, supervised students and edited the manuscript. M.J.E. performed electrophysiological experiments. A.K. performed electrophysiological experiments and data analyses. A.S. performed immunohistochemistry experiments and contributed to the writing of the manuscript. M.L.-C. and A.T.-B. contributed to behavioural tests. S.B. performed data analyses. G.M.R., S.S. and N. Salmaso contributed to experimental design, data analysis and manuscript editing. G.G., J.-C.L. and N. Sonenberg supervised students, designed experiments and contributed to writing the manuscript.

Competing interests The authors declare no competing interests.

Additional information
Supplementary information is available for this paper at https://doi.org/10.1038/s41586-020-03047-0.
Correspondence and requests for materials should be addressed to A.A.-V. or N. Sonenberg.
Peer review information *Nature* thanks Kimberly Raab-Graham and the other, anonymous, reviewer(s) for their contribution to the peer review of this work.
Reprints and permissions information is available at http://www.nature.com/reprints.

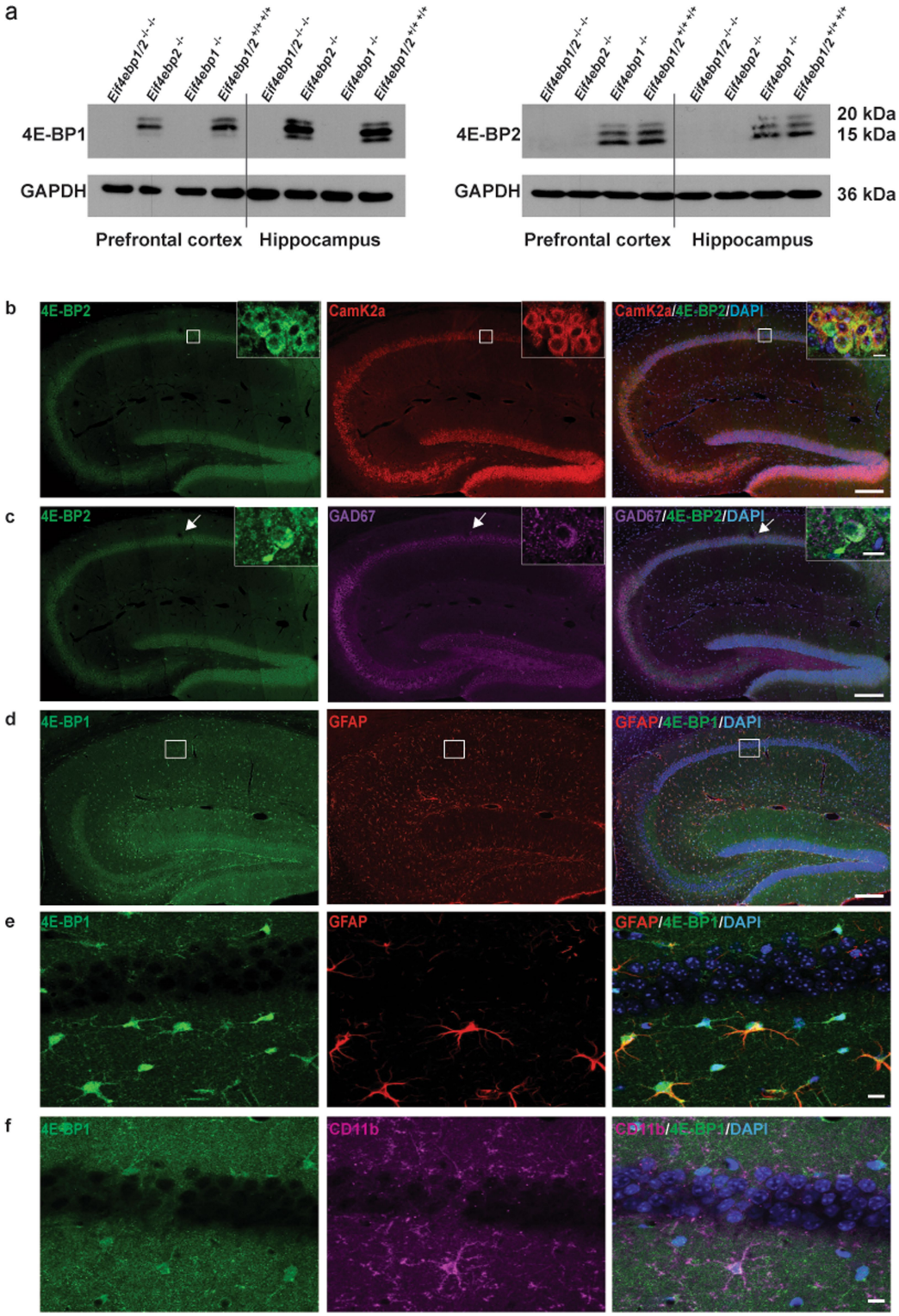

Extended Data Fig. 1 | Expression of 4E-BP1 and 4E-BP2 in the prefrontal cortex and hippocampus. a, Representative western blot analysis (from 3 independent experiments) of 4E-BP1 and 4E-BP2 in the prefrontal cortex and hippocampus of wild-type (*Eif4ebp1/2*$^{+/+/+/+}$), 4E-BP1 knock out (*Eif4ebp1*$^{-/-}$), 4E-BP2 knock out (*Eif4ebp2*$^{-/-}$), and 4E-BP1/2 double knock out mice (*Eif4ebp1/2*$^{-/-}$) (uncropped blots are presented in Supplementary Information). **b**, **c**, Representative confocal images of immunostaining for 4E-BP2 (green), CAMK2α (red)/GAD67 (magenta) in the hippocampus. The arrows indicate area showed in the insert, which is a higher magnification of the images. Insert scale bar: 10 µm. Brain sections were additionally counterstained with DAPI (blue). **d**, Representative confocal images of immunostaining for 4E-BP1 (green), GFAP (red) in the hippocampus. Brain sections were additionally counterstained with DAPI (blue). The white box indicates area shown in **e**. **f**, Representative confocal image of immunostaining for 4E-BP1 (green) and CD11b (magenta). Brain sections were additionally counterstained with DAPI (blue). All immunofluorescence experiments were repeated in 3 independent experiments.

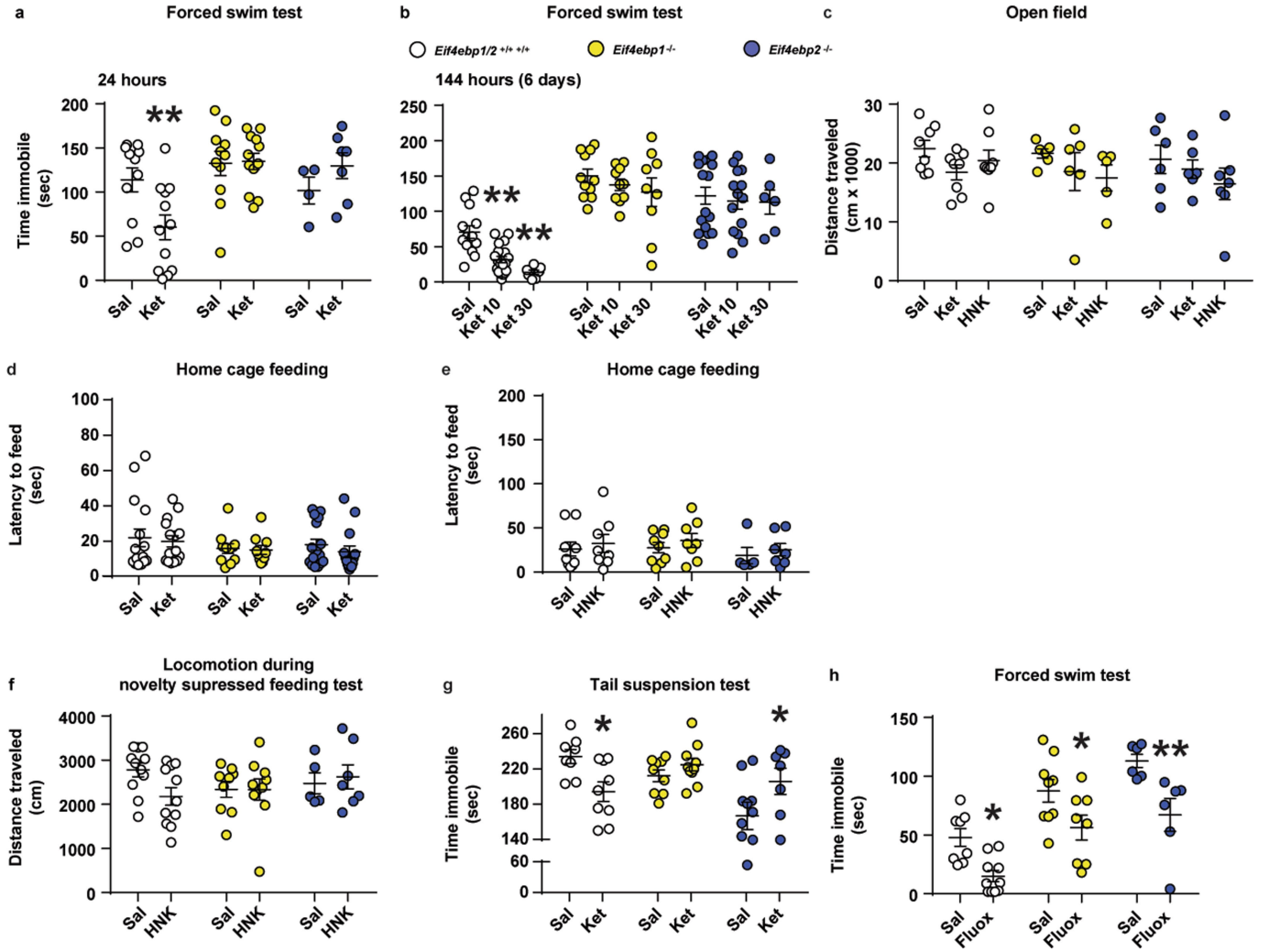

Extended Data Fig. 2 | 4E-BP1 and 4E-BP2 are required for the antidepressant effect of ketamine. a, A group of *Eif4ebp1/2*$^{+/+}$, *Eif4ebp1*$^{-/-}$ and *Eif4ebp2*$^{-/-}$ mice were treated with saline or ketamine (IP, 10 mg kg^{-1}) and tested 24 h after injection in the FST (2-way ANOVA and Fisher's LSD, $n = 11, 13, 11, 12, 4, 7$ from left to right). **b**, Wild-type (*Eif4ebp1/2*$^{+/+}$), *Eif4ebp1*$^{-/-}$ and *Eif4ebp2*$^{-/-}$ mice were treated with saline or ketamine (IP, 10 or 30 mg kg^{-1}) and tested in the FST 6 days after treatment (2-way ANOVA and Fisher's LSD, $n = 13, 19, 7, 11, 10, 9, 16, 14, 6$ from left to right). **c**, A different group of mice treated as in **a** was tested in the open field, and general activity was measured as distance travelled (2-way ANOVA, $n = 8, 8, 8, 6, 6, 5, 6, 6, 7$ from left to right). **d**, Latency to feed in the home cage was measured immediately after the NSF task in *Eif4ebp1/2*$^{+/+ +/+}$, *Eif4ebp1*$^{-/-}$ and *Eif4ebp2*$^{-/-}$ mice, treated with saline or Ket (corresponding to Fig. 1b; 2-way ANOVA). **e**, Latency to feed in the home cage was also measured after the NSF task in the three mouse strains, following saline or (2R,6R)-HNK treatment (corresponding to Fig. 1c; 2-way ANOVA). **f**, In the same group of mice as in **e** (and Fig. 1c) average distance travelled during the NSF test was measured (expressed as an average per minute to correct for differential time spent in the arena; 2-way ANOVA). **g**, Mice of the three genotypes were also tested for immobility in the tail suspension test, 1 h after saline or Ket treatments (2-way ANOVA and Fisher's LSD, $n = 8, 9, 9, 10, 10, 7$ from left to right). **h**, *Eif4ebp1/2*$^{+/+ +/+}$, *Eif4ebp1*$^{-/-}$ and *Eif4ebp2*$^{-/-}$ mice were treated with fluoxetine (Fluox, IP, 3 mg kg^{-1}, 0.5 h) and tested in the FST (2-way ANOVA and Fisher's LSD, $n = 8, 10, 9, 8, 6, 6$ from left to right). Mean ± s.e.m.; * $P < 0.05$; ** $P < 0.01$ vs. Sal-treated mice of the same genotype.

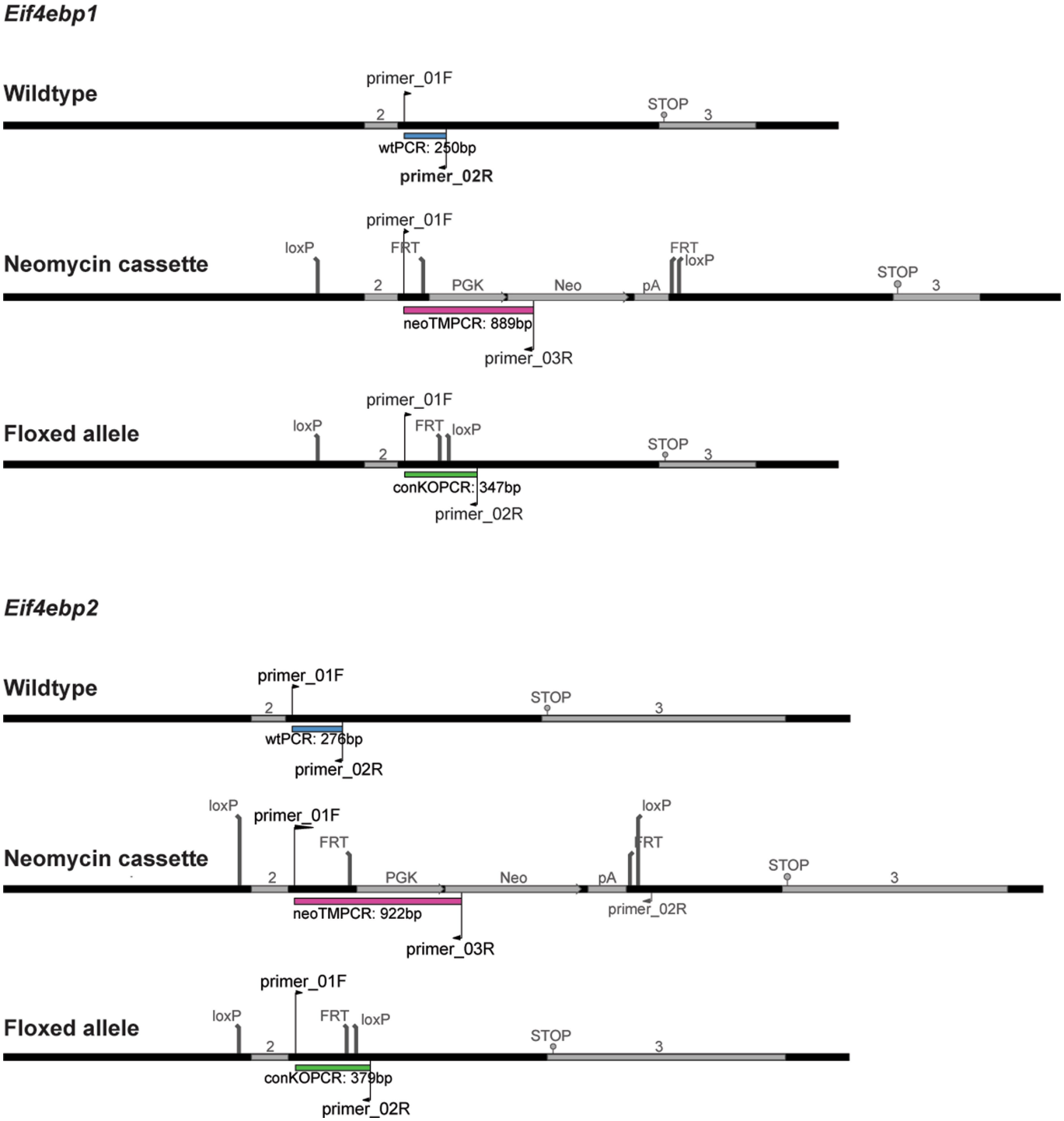

Extended Data Fig. 3 | Generation of *Eif4ebp1* and *Eif4ebp2* floxed genes in mice. Schematic representation of the targeting construct used for the generation of *Eif4ebp1* and *Eif4ebp2* knockout mice. FRT (FLPase recognition target) and loxP sequences are indicated. Positive (PGK-neo) selection markers are indicated in the schemes on the Neomycin cassette (Neo, neomycin). Numbered grey boxes represent exons in the *Eif4ebp1* and *Eif4ebp2* genes. The *Eif4ebp1* and *Eif4ebp2* neomycin alleles were produced by homologous recombination. FLPase was used to generate the *Eif4ebp1* and *Eif4ebp2* floxed alleles. The genotyping PCR primers are indicated for each construct, as well as the length of the PCR product.

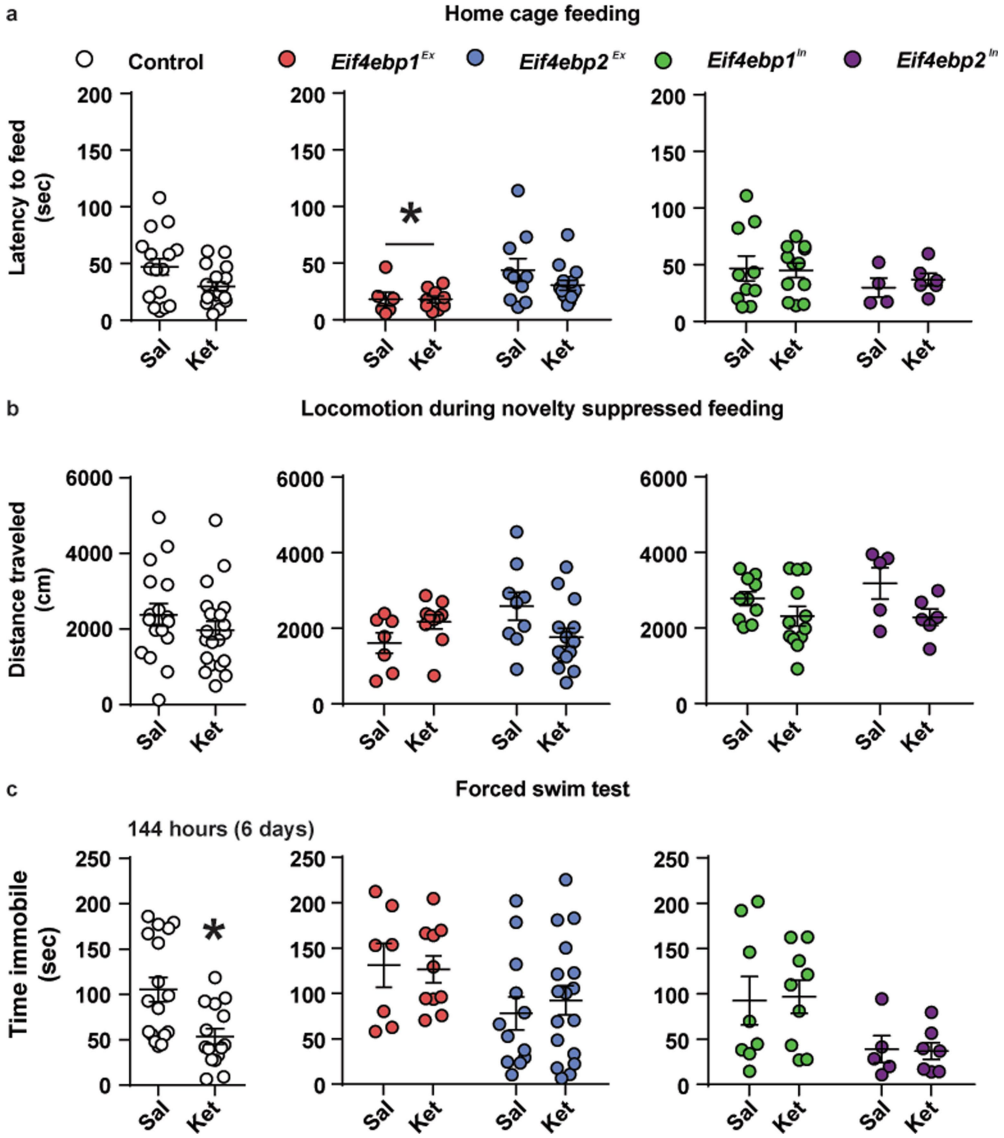

Extended Data Fig. 4 | Effects of cell-specific mutation of *Eif4ebp1* and *Eif4ebp2* on home cage feeding, locomotion and forced swim test. **a**, Latency to feed in the home cage was measured 1 h after saline or Ket (IP, 10 mg kg^{-1}) treatments in control, mice lacking *Eif4ebp1* in CAMK2α^{+} (*Eif4ebp1*^{Ex}) or GAD2^{+} neurons (*Eif4ebp1*^{In}), or mice mutant for *Eif4ebp2* in excitatory (*Eif4ebp2*^{Ex}) or inhibitory (*Eif4ebp2*^{In}) neurons (corresponding to mice in Fig. 2i; 2-way ANOVA and Dunnett's). **b**, In these same mice, distance travelled during the NSF task was measured. Data were expressed as average distance travelled per minute to account for differences in latency to feed (2-way ANOVA and Dunnett's). **c**, Control, *Eif4ebp1*^{Ex}, *Eif4ebp1*^{In}, *Eif4ebp2*^{Ex} and *Eif4ebp*^{In} mice were tested 6 days (144 h) after saline or Ket treatment (IP, 10 mg kg^{-1}) in the FST (2-way ANOVA and Fisher's LSD, $n = 17, 15, 7, 10, 12, 17, 8, 9, 5, 7$ from left to right). Mean ± s.e.m.; * $P < 0.05$ vs. control (main effect of genotype, in a) or vs. Sal-treated mice of the same genotype.

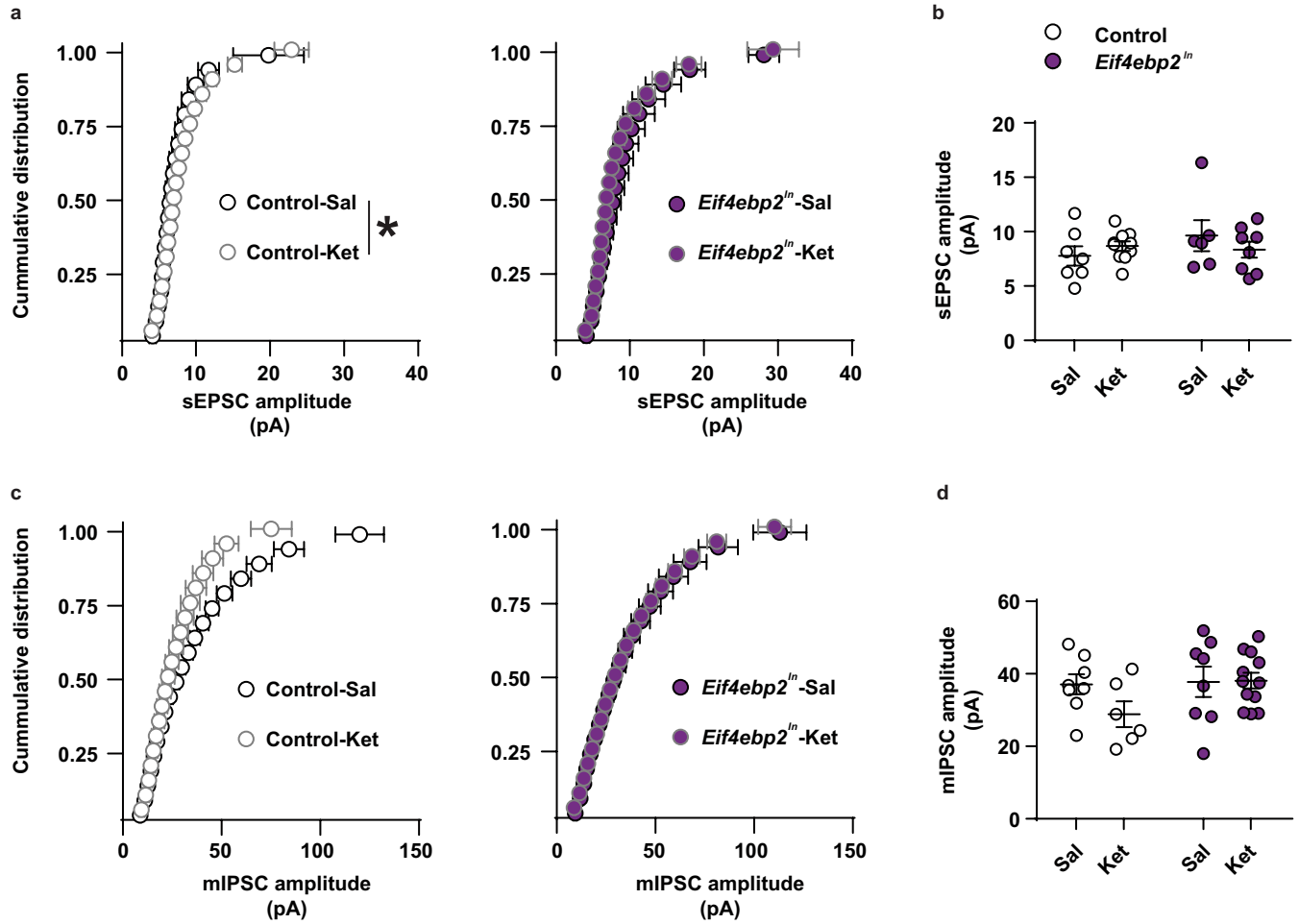

Extended Data Fig. 5 | Effects of 4E-BP2 mutation in inhibitory neurons on amplitude of sEPSC and mIPSC. a, Cumulative distribution of sEPSC amplitude in CA1 pyramidal neurons of control and *Eif4ebp2*^{In} mice treated with saline or Ket (mice recorded in Fig. 3; Kolmogorov–Smirnov test). **b**, Amplitude of sEPSCs recorded from pyramidal neurons in CA1 of control and *Eif4ebp2*^{In} mice (mice recorded in Fig. 3; 2-way ANOVA). **c**, Cumulative distribution of mIPSC amplitude in CA1 pyramidal neurons from mice treated as in **a** (mice recorded in Fig. 4; Kolmogorov–Smirnov test). **d**, Amplitude of mIPSC in CA1 pyramidal neurons in mice treated as in **a** (mice recorded in Fig. 4; 2-way ANOVA). Mean ± s.e.m.; * $P < 0.05$ vs. control-Sal.

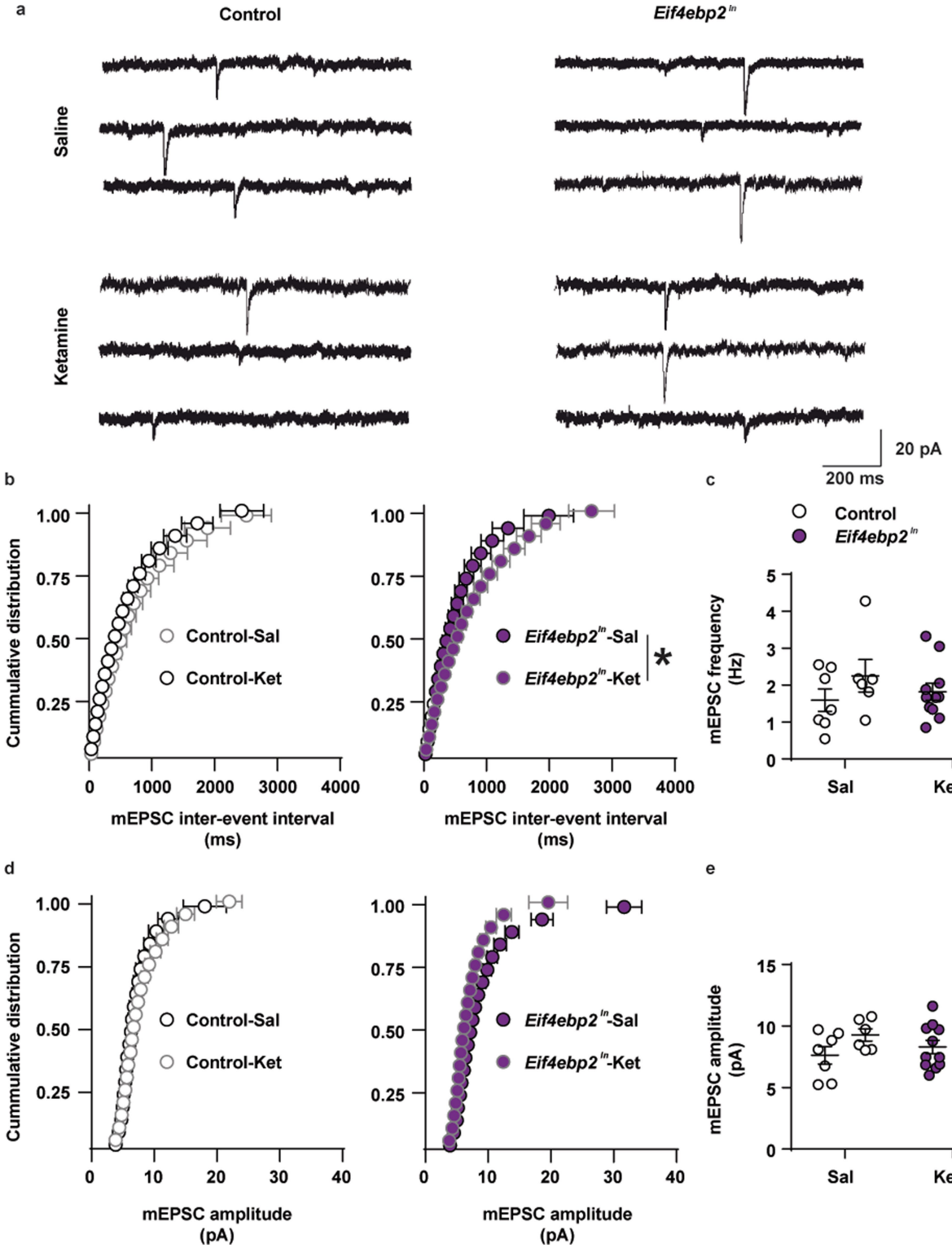

Extended Data Fig. 6 | The absence of 4E-BP2 in inhibitory neurons does not affect mEPSCs in pyramidal neurons. a, Representative whole-cell recordings of mEPSCs in CA1 pyramidal neurons of mice treated with saline or Ket 24 h before (IP, 10 mg kg^{-1}). Control and *Eif4ebp2*^{In} mice were used. **b**, Cumulative inter-event interval (Kolmogorov–Smirnov test, $n = 7, 11, 6, 17$ from left from right) and **c**, frequency of mEPSCs measured in **a** (2-way ANOVA). **d**, Cumulative (Kolmogorov–Smirnov test) and **e**, average distribution of mEPSC amplitude measured in **a** (2-way ANOVA). Mean ± s.e.m.; * $P < 0.05$ vs. *Eif4ebp2*^{In}-Sal.

nature research

Corresponding author(s): Argel Aguilar-Valles, Nahum Sonenberg

Last updated by author(s): Sep 9, 2020

Reporting Summary

Nature Research wishes to improve the reproducibility of the work that we publish. This form provides structure for consistency and transparency in reporting. For further information on Nature Research policies, see our Editorial Policies and the Editorial Policy Checklist.

Statistics

For all statistical analyses, confirm that the following items are present in the figure legend, table legend, main text, or Methods section.

n/a	Confirmed	
☐	☒	The exact sample size (*n*) for each experimental group/condition, given as a discrete number and unit of measurement
☐	☒	A statement on whether measurements were taken from distinct samples or whether the same sample was measured repeatedly
☐	☒	The statistical test(s) used AND whether they are one- or two-sided *Only common tests should be described solely by name; describe more complex techniques in the Methods section.*
☒	☐	A description of all covariates tested
☐	☒	A description of any assumptions or corrections, such as tests of normality and adjustment for multiple comparisons
☐	☒	A full description of the statistical parameters including central tendency (e.g. means) or other basic estimates (e.g. regression coefficient) AND variation (e.g. standard deviation) or associated estimates of uncertainty (e.g. confidence intervals)
☐	☒	For null hypothesis testing, the test statistic (e.g. *F*, *t*, *r*) with confidence intervals, effect sizes, degrees of freedom and *P* value noted *Give P values as exact values whenever suitable.*
☒	☐	For Bayesian analysis, information on the choice of priors and Markov chain Monte Carlo settings
☒	☐	For hierarchical and complex designs, identification of the appropriate level for tests and full reporting of outcomes
☒	☐	Estimates of effect sizes (e.g. Cohen's *d*, Pearson's *r*), indicating how they were calculated

Our web collection on statistics for biologists contains articles on many of the points above.

Software and code

Policy information about availability of computer code

Data collection	Behaviour acquisition: Videotrack, View Point Life Science. Imaging: Zeiss ZEN 3.2. Field and whole-cell recording of synaptic currents: pClamp 10
Data analysis	Electrophysiology analyses: Clampfit 10.6 and MIni Analysis 6.0. Statistical analyses :GraphPad Prism 6

For manuscripts utilizing custom algorithms or software that are central to the research but not yet described in published literature, software must be made available to editors and reviewers. We strongly encourage code deposition in a community repository (e.g. GitHub). See the Nature Research guidelines for submitting code & software for further information.

Data

Policy information about availability of data

All manuscripts must include a data availability statement. This statement should provide the following information, where applicable:

- Accession codes, unique identifiers, or web links for publicly available datasets
- A list of figures that have associated raw data
- A description of any restrictions on data availability

All data generated or analysed during this study are included in this published article and its supplementary information files.

Field-specific reporting

Please select the one below that is the best fit for your research. If you are not sure, read the appropriate sections before making your selection.

☒ Life sciences ☐ Behavioural & social sciences ☐ Ecological, evolutionary & environmental sciences

For a reference copy of the document with all sections, see nature.com/documents/nr-reporting-summary-flat.pdf

Life sciences study design

All studies must disclose on these points even when the disclosure is negative.

Sample size	Group size estimates were based on previous experience with the experimental design and mouse models. We aimed for a group size of 8-12 (per genotype per treatment) for behavioral experiments and 6-8 for Western blot and electrophysiologycal recordings. In several cases, especially for wildtype mice, these group sizes exceeded these numbers, since several batches of mice were tested independently and pooled together for final analyses.
Data exclusions	No data were excluded from analyses.
Replication	All experiments were replicated at least 3 times and all attempts were successful.
Randomization	Age-matched animals from each genotype were randomly allocated into each experimental group.
Blinding	Behavioral tests were scored using a software (Videotrack, View Point Life Science, Montreal, Canada) by a researcher blind to treatment and genotype. Electrophysiological data were analyzed offline by a researcher blind to treatment and genotype. Western blots and IF were are analyzed by a researcher bind to the genotypes.

Reporting for specific materials, systems and methods

We require information from authors about some types of materials, experimental systems and methods used in many studies. Here, indicate whether each material, system or method listed is relevant to your study. If you are not sure if a list item applies to your research, read the appropriate section before selecting a response.

Materials & experimental systems

n/a	Involved in the study
☐	☒ Antibodies
☒	☐ Eukaryotic cell lines
☒	☐ Palaeontology and archaeology
☐	☒ Animals and other organisms
☒	☐ Human research participants
☒	☐ Clinical data
☒	☐ Dual use research of concern

Methods

n/a	Involved in the study
☒	☐ ChIP-seq
☒	☐ Flow cytometry
☒	☐ MRI-based neuroimaging

Antibodies

Antibodies used

Antibody - Supplier - Catalogue number - Clone name - Lot number
Anti 4E-BP1 - Cell Signaling Technology - 9644S - 53H11
Anti 4E-BP2 - Cell Signaling Technology - 2845S - N/A - Lot #4
Anti-GAPDH-HRP - Abcam - ab9482 - mAbcam 9484
Anti CaMKII-α - Cell Signaling Technology - 50049S - 6G9
Anti Gad67 - EMD Millipore - MAB5406B - 1G10.2
Anti GFAP - Cell Signaling Technology - 3670S - GA5
Anti CD11b - BioRad - MCA711 - 5C6

Goat anti-Rabbit IgG (H+L) Cross-Adsorbed Secondary Antibody, HRP- Thermo Fisher Scientific - G-21234

Alexa Fluor 488 goat anti-rabbit IgG - Thermo Fisher Scientific - A11034 - N/A
Alexa Fluor 546 goat anti-mouse IgG - Thermo Fisher Scientific - A10036 - N/A
Alexa Fluor 647 streptavidin conjugate - Thermo Fisher Scientific - S21374 - N/A
Alexa Fluor 647 goat anti-rat IgG - Thermo Fisher Scientific - A-21247 -N/A

Validation

Anti-4E-BP1. In the current manuscript (Extended Data Fig. 3) and in previous publications (i.e. Tsukiyama-Kohara, et al Nat Medicine 2001; Banko, et al J Neuro, 2005), we have observed that the signal 4E-BP1 is absent in Eif4ebp1-/- and intact in Eif4ebp2-/- mice.
Anti-4E-BP2. In the current manuscript (Extended Data Fig. 3) and in previous publications (i.e. Tsukiyama-Kohara, et al Nat Medicine

2001; Banko, et al J Neuro, 2005), we have observed that the signal 4E-BP2 is absent in Eif4ebp2-/- and intact in Eif4ebp1-/- mice.
Anti-GAPDH. Validated by Abcam, as per the company's website (https://www.abcam.com/gapdh-antibody-mabcam-9484-loading-control-ab9484.html).
Anti-CaMKII-α. Validated by Cell Signaling Technology, used for immunofluorescence in mouse tissue in Liu, et al Sci Rep, 2017.
Anti-Gad67. Validated by Millipore Sigma, used in over 10 studies as per company's website (https://www.emdmillipore.com/CA/en/product/Anti-GAD67-Antibody-clone-1G10.2,MM_NF-MAB5406#documentation)
Anti-GFAP. Validated by Cell Signaling Technology, used for immunofluorescence in mouse tissue in several studies as per the company's website (https://www.cellsignal.com/products/primary-antibodies/gfap-ga5-mouse-mab/3670?site-search-type=Products&N=4294956287&Ntt=3670s&fromPage=plp&_requestid=2185529).
Anti-CD11b. Validated for immunofluorescence by Bio-Rad, used in >40 studies as per the company's website (https://www.bio-rad-antibodies.com/monoclonal/mouse-cd11b-antibody-5c6-mca711.html?f=purified#references).

Animals and other organisms

Policy information about studies involving animals; ARRIVE guidelines recommended for reporting animal research

Laboratory animals	Adult male mice (P60-180) were used. We used constitutive (i.e. full-body) mutant mice for Eif4ebp1-/- and Eif4ebp2-/- and their wiltype littermates. Eif4ebp1f/f and Eif4ebp2f/f were generated by Ozgene Pty Ltd (Perth, Australia). Conditional knockouts were generated by crossing Eif4ebp1f/f and Eif4ebp2f/f mice with either Camk2a-cre (Jackson Laboratories stock No: 005359) or Gad2-cre (Jackson Laboratories stock number: 010802) mice.
Wild animals	The study did not involve wild animals.
Field-collected samples	The study did not involve samples collected in the field.
Ethics oversight	All procedures followed the Canadian Council on Animal Care guidelines and were approved by McGill University and Université de Montréal Animal Care Committees.

Note that full information on the approval of the study protocol must also be provided in the manuscript.